SOLAR THERMAL ENERGY DRIVEN ORGANIC RANKINE CYCLE SYSTEMS FOR ELECTRICITY AND FRESH WATER GENERATION

Nishith B. Desai[1]*, Henrik Pranov[2], Fredrik Haglind[3]

[1]Technical University of Denmark, Department of Mechanical Engineering,
2800 Kongens Lyngby, Denmark
nbdes@mek.dtu.dk

[2]Heliac ApS
Hørsholm, Denmark
hjp@heliac.dk

[1]Technical University of Denmark, Department of Mechanical Engineering,
2800 Kongens Lyngby, Denmark
frh@mek.dtu.dk

* Corresponding Author

ABSTRACT

For small to medium scale dispatchable (on demand) power and fresh water generation, solar photovoltaic with battery storage using reverse osmosis and diesel generator based systems can be used. Both options are costly, and in addition, while the former generates highly saline wastewater, the latter results in the production of greenhouse gasses. A more attractive option is, therefore, to use systems driven by solar thermal energy consisting of solar collectors, a power cycle and a thermal energy driven fresh water generation system. However, currently used concentrated solar power technologies (parabolic trough collector, linear Fresnel reflector, solar power tower) use heavy and very expensive glass mirrors and receivers. Recently, a novel polymer foil-based concentrating solar collector system, which avails the advantages of low installation cost, two-axis tracking and low operation and maintenance cost, has been proposed. A techno-economic analysis of a foil-based concentrating solar collector powered organic Rankine cycle based electricity and thermal energy driven fresh water generation system is presented in this paper. Specifically, the objective is to identify which is the more appropriate working fluid for such plant. The results indicate that cyclopentane is the more appropriate organic working fluid, compared to n-pentane, isopentane, hexamethyldisiloxane and toluene, for foil-based solar power plants.

1. INTRODUCTION

Energy (including electricity) and water are intricately connected. An integrated development of the energy and water supply policies is of vital importance for development of locations with water scarcity. Commonly used small to medium scale systems (few kW to few MW) for simultaneous generation of power and fresh water include solar photovoltaic system using reverse osmosis (RO) and diesel generator based systems using RO for fresh water generation. For dispatchable cogeneration, solar photovoltaic system with battery storage can be used. However, the large battery systems are expensive despite large volume production already in place and it has yet to be proven that batteries will ever become cheap and durable enough to become profitable for large-scale energy storage. Patil et al. (2017) presented that the levelized cost of electricity (LCOE) for solar photovoltaic systems with battery storage is about 36.8 % higher than that of the parabolic trough collector powered organic Rankine cycle system with thermal energy storage. Shalaby (2017)

reported that concentrated solar energy powered organic Rankine cycle based desalination systems are better in terms of their techno-economic performance compared to solar photovoltaic powered desalination systems. It is not recommended to use solar photovoltaic system with batteries to drive RO desalination system because of the high capital and running cost (Shalaby, 2017). Diesel generator based systems are typically used in isolated regions and islands. In such cases, as the diesel is imported from the nearby port, the cost of electricity generated from the diesel generator sets is high (Bandyopadhyay and Desai, 2017). With respect to concentrated solar power (CSP) based electricity and fresh water generation systems, steam Rankine cycle systems (Palenzuela *et al.*, 2015), organic Rankine cycle (ORC) systems (Astolfi *et al.*, 2017), or supercritical carbon dioxide Brayton cycle (Sharan *et al.*, 2019) can be used for power generation, and reverse osmosis systems (El-Emam and Dincer, 2018) or thermally driven desalination systems (Astolfi *et al.*, 2017) can be used for fresh water generation.

Hoffmann and Dall (2018) presented that the LCOE for solar power tower integrated Rankine cycle increases by 8.8 % when used for co-generation. This is because the condensing stream leaving the turbine should be at a higher temperature to act as an energy source for the cogeneration application. The revenue generated from the other product (heat, fresh water, or cooling) may compensate for this low efficiency and high cost of electricity. The concentrated solar power integrated multi-effect distillation (MED) system is a cheaper option compared to a RO system (Ghobeity *et al.*, 2011). The specific electricity consumption for RO system is 3.5 kWh_e/m^3 to 5 kWh_e/m^3, depending on many factors like sea water salinity, component efficiencies, membrane configuration, etc. (IRENA, 2012; Sharan *et al.*, 2019). The specific electricity consumption for MED based seawater desalination system is 1 kWh_e/m^3 to 1.5 kWh_e/m^3 (Alfa Laval, 2018). The RO system also has a low recovery ratio. One commercial solar power tower based plant with steam Rankine cycle system and a thermally driven desalination unit was recently put into operation in Australia (NREL, 2019). Sharan *et al.* (2019) reported that the cost of distillate produced by a plant consisting of a solar power tower and a super critical carbon dioxide Brayton cycle integrated with a MED system is 16 % lower than the distillate produced by a RO system for Yanbu, Saudi Arabia.

For small to medium scale applications, ORC based cogeneration systems are preferred over other power cycles. For CSP integrated ORC system with RO desalination, toluene (Delgado-Torres *et al.*, 2007), isopentane (Bruno *et al.*, 2008), R134a (Karellas *et al.*, 2011), hexamethyldisiloxane (MM) (Li *et al.*, 2013), and n-octane (El-Emam and Dincer, 2018) were proposed as promising working fluids. Toluene (Sharaf, 2012), cyclo-pentane (Mathkor *et al.*, 2015), n-pentane (Astolfi *et al.*, 2017) were proposed as the preferred choice for CSP integrated ORC systems with thermal desalination. The parabolic trough collector (PTC) is the most widely used solar concentrator for ORC based cogeneration systems (El-Emam and Dincer, 2018, Sharaf, 2012). The assumptions related to the solar radiation, capital cost of the sub-systems and electricity consumption influence the techno-economic performance of the cogeneration system significantly. It is worth to note that the PTC system cost assumed in most of the previous works is based on a typical 50 MW_e CSP plant. However, it is difficult to get the PTC field with same cost at low capacities (e.g. around 1 MW_e). The conservative estimates of the sub-system costs leads to low cost estimates for the power and fresh water generation. Currently used CSP technologies use heavy and very expensive glass mirrors and receivers. Therefore, these technologies are only suitable for large-scale installations in regions with high annual direct normal irradiance (DNI). Recently, a cost-effective polymer foil-based novel concentrating solar power system, which uses a focusing plastic film that is adhered to a glass plate, has been proposed. This system also avails the advantages of two-axis tracking and low operation and maintenance cost. Desai *et al.* (2019) presented a comparison between the foil-based and PTC-based CSP plants with an ORC power system. The results suggested that the foil-based CSP plant can reduce the LCOE by up to about 40 % compared to parabolic trough collector based plants. There are no other previous papers addressing the foil-based concentrating solar power system.

A techno-economic analysis of a foil-based CSP powered ORC based electricity and thermal energy driven fresh water generation system is presented in this paper. Specifically, the objective is to

identify which is the more appropriate working fluid for such plant. Five different working fluids, cyclopentane, n-pentane, isopentane, toluene, and MM, were considered in the analysis.

2. METHODS

2.1 System description

A simplified schematic of the foil-based CSP system for electricity and fresh water generation is given in Figure 1. The foil-based solar collector concentrates solar energy on the receiver and the collected thermal energy is used to produce electricity through the power cycle. The energy available at the exhaust of turbine is utilized for a thermal energy driven desalination system. The system is equipped with a conventional two-tank molten salt-based energy storage system.

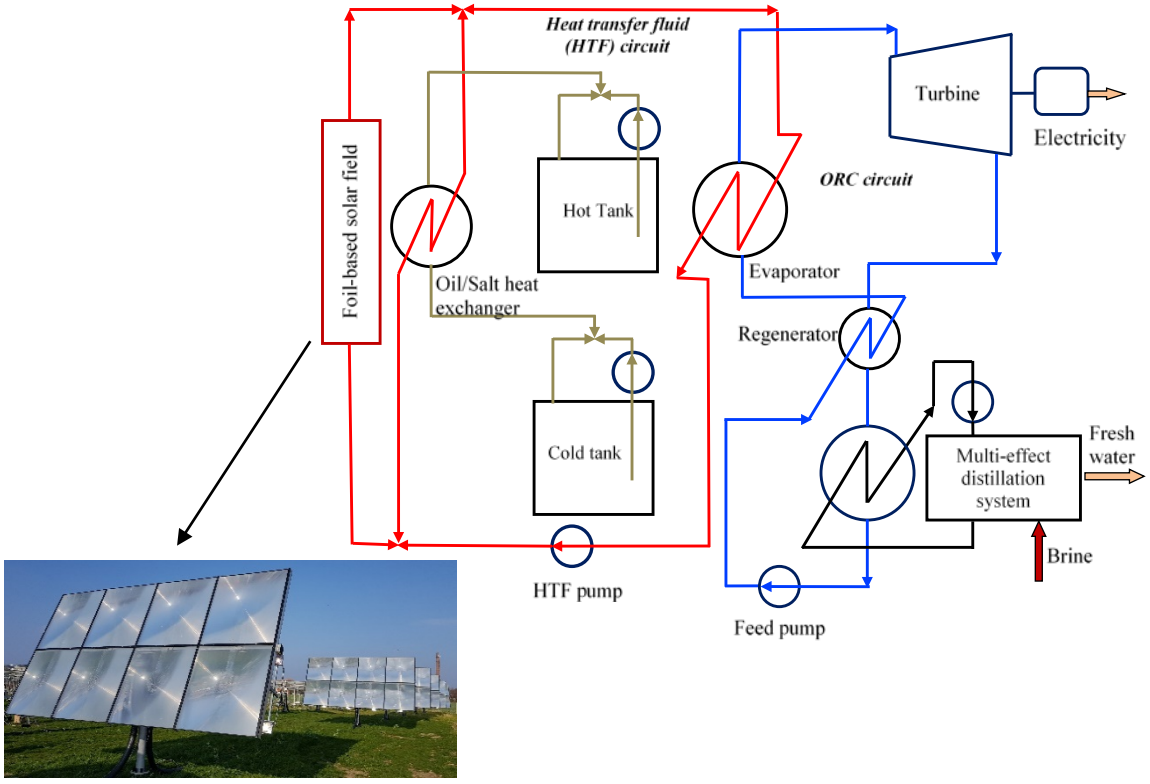

Figure 1: Foil-based solar collector powered organic Rankine cycle and multi-effect desalination system

2.2 Concentrating solar field

The concentrating solar field useful energy gain (Q_{CL}) is calculated as follows:

$$Q_{CL} = \eta_{o,CL} \cdot DNI \cdot IAM \cdot A_{p,CL} - U_l \cdot \left(T_{m,CL} - T_a\right) \cdot A_{p,CL} \quad (1)$$

where $\eta_{o,CL}$ is the solar collector field's optical efficiency, U_l is the heat loss co-efficient based on the aperture area of the solar collector field, $T_{m,CL}$ is the mean temperature of solar collector field, T_a is the ambient temperature, and DNI is the direct normal irradiance. The incidence angle modifier (IAM) for the foil-based solar field is one because of the two-axis tracking. The shadow losses and end-losses are neglected in the analysis, which are typically calculated based on the solar field layout prepared during the detailed engineering design stage. The value of these losses is small about 3% (Heller, 2017). The heat losses and pressure drop through piping (typically, calculated during detailed engineering design stage) are also neglected in the analysis. A penalty in net annual energy output for start-up/shut-down and other losses was considered in the analysis.

2.3 Organic Rankine cycle power system

The power output of the turbine at design condition (P_D) and the gross peak plant electric output at design condition ($P_{gross,D}$) is calculated as follows:

$$P_D = \dot{m}_D \cdot \Delta h_{is,D} \cdot \eta_{is,D} \quad \text{and} \quad P_{gross,D} = P_D \cdot \eta_{g,D} \tag{2}$$

where $\dot{m}_D$ is the mass flow rate of the organic fluid at design conditon, $\eta_{is,D}$ is the isentropic efficiency of turbine at design condition, $\Delta h_{is,D}$ is the isentropic enthalpy change in the turbine at design condition, and $\eta_{g,D}$ is the generator efficiency at design condition.

The power output of turbine power (P) and power system mass flow rate ($\dot{m}$) relationship can be assumed as a linear relation (Willans line equation) over a reasonable range [14]:

$$P = a + b \cdot \dot{m} \tag{3}$$

$$a = -y \cdot P_D \; and \; b = (1 + y) \cdot \Delta h_{is,D} \cdot \eta_{is,D} \tag{4}$$

The value of power input at zero flow to maintain the speed (internal losses of turbine), a, was calculated based on the expression given by Mavromatis and Kokossis (1998) and the value of slope, b, was calculated based on the expression given by Desai *et al.* (2014).

The UA value for heat exchangers at part-load conditions is given as follows (Patnode, 2006):

$$\frac{\dot{m}}{\dot{m}_D} = \left(\frac{UA}{UA_D}\right)^{0.8} \tag{5}$$

At part-load, the generator efficiency was assumed to vary as follows (Haglind and Elmegaard, 2009):

$$\eta_g = \frac{\eta_{g,D} \cdot \left(\frac{P}{P_D}\right)}{\eta_{g,D} \cdot \left(\frac{P}{P_D}\right) + \left[\left(1 - \eta_{g,D}\right) \cdot \left((1 - F_{cu}) + F_{cu} \cdot \left(\frac{P}{P_D}\right)^2\right)\right]} \tag{6}$$

where F_{cu} is the copper loss fraction and a value of 0.43 was assumed (Haglind and Elmegaard, 2009).

The part-load efficiency of the ORC system pump was estimated using a polynomial expression extracted from Veres (1994):

$$\eta_P = \eta_{P,D} \cdot \left[-0.029265 \cdot \left(\frac{\dot{V}}{\dot{V}_D}\right)^3 - 0.14086 \cdot \left(\frac{\dot{V}}{\dot{V}_D}\right)^2 + 0.3096 \cdot \left(\frac{\dot{V}}{\dot{V}_D}\right) + 0.86387\right] \tag{7}$$

where $\dot{V}$ is volume flow rate at the inlet of pump and $\eta_{P,D}$ is the pump efficiency at design condition. The change of pump efficiency with rotational speed was neglected.

2.4 Thermal energy storage

Both thermal energy storage tanks are modelled as a well-mixed tank. The variations in the UA value for the storage tank (UA_{Tank}) was calculated as follows (Herrmann *et al.*, 2004):

$$UA_{Tank} = a_{Tank} \cdot T_{salt} + b_{Tank} \tag{8}$$

where T_{salt} is the salt temperature in the tank, a_{Tank} and b_{Tank} are the experimentally derived parameters for the molten salt based storage tank.

2.5 Economic analysis

The annualized cost (AC) was calculated as follows:

$$AC_{sys} = \left(C_{sys} \cdot CRF + C_{O\&M}\right) \quad and \quad CRF = d \cdot \frac{(1 + d)^k}{((1 + d)^k) - 1} \tag{9}$$

where C_{sys} is the capital cost of complete system, $C_{O\&M}$ is the annual operation and maintenance cost, *CRF* is the capital recovery factor, *d* is the discount rate, and *k* is the lifetime.
The levelized cost of fresh water generation (LCOW) was calculated as follows:

$$LCOW = \frac{AC_{sys} - (LCOE \cdot E_{annual,net})}{V_{annual,net}} \tag{10}$$

$$LCOE = \frac{AC_{sys,only\ power}}{E_{annual,net,only\ power}} \tag{11}$$

where $V_{annual,net}$ is the net annual fresh water generation and $E_{annual,net}$ is the net annual electricity generation for the cogeneration system. The LCOE was calculated considering only power generation (with condensing turbine). When the system is used for cogeneration, the condensing pressure is increased based on the MED system requirements. This leads to decrease in the thermal efficiency of ORC system and increase in the solar field area for the same power output (1 MW_e). In addition to the MED system cost, the cost of solar field, storage system and ORC system increase in case of cogeneration.

3. RESULTS AND DISCUSSION

The techno-economic analyses of the proposed system were performed using the Engineering Equation Solver (EES) (Klein, 2018). DNI and ambient temperature data for the place Cape Town (South Africa) were taken from US DOE (2014) and annual simulations were performed. The solar field performance characteristics for the foil-based system were provided by Heliac ApS, Denmark. The ORC power system code has been validated using data of a plant using n-pentane located in USA, Arizona Public Service Saguaro plant (NREL, 2018), and a manufacturer catalogue (Turboden, 2018) (Desai *et al.*, 2019). The value of fraction of internal losses of turbine (*y*) is taken as 0.12. For loads down to 40 %, the maximum absolute deviation in gross thermal efficiency of the ORC is 0.5 %-points and 0.28 %-points for n-pentane and MM, respectively. The maximum absolute deviation in gross thermal efficiency for loads below 40 % is 2.2 % and 1 % for n-pentane and MM, respectively. In the present work, the CSP plant was modelled with a thermal energy storage (9 h capacity) and during low radiation the stored energy is used in such a way that the plant operates near full load. Therefore, it is rare that the ORC power system operates at loads lower than 40 %.

The design isentropic efficiency of the turbine was calculated based on the correlation given by Astolfi and Macchi (2015). For n-pentane and MM, it is observed that the design isentropic efficiencies based on the correlation is higher compared to the actual efficiencies given for the plants. This observation agrees with the results reported by Hasselmann *et al.* (2014). In this work the most widely used organic working fluids for medium temperature and medium-scale applications in previous works, for CSP based electricity and fresh water generation, cyclopentane, n-pentane, isopentane, toluene, and MM, were considered. As the capital cost of the toluene-based system is much higher than those of the other working fluids, it was discarded for further investigations. The data given in Table 1 and Table 2 were used for the analysis. The receiver for the current foil-based solar collector field is optimized for the district heating applications, and there is a significant potential for improvement of its thermal performance. In addition to that, foil-based concentrating solar collectors are easy to produce compared to the conventional mirror based concentrating solar collectors. High production rates and use of standard components in the system, ensure scalability as well as security of supply. Therefore, for future foil-based CSP plants, a high cost reduction potential exist. The analysis of the foil-based collector powered ORC integrated MED system, considering medium to large-scale production cost (150 €/m^2) and 20 % improvement in the heat-loss coefficient of the receiver, is also presented.

Rayegan and Tao (2011) have suggested a procedure for determining the highest limit of the evaporation pressure for the ORC working fluid. In the present work, considering the safety margin, the maximum evaporation temperature of the ORC working fluid was taken as 10 °C lower than the

Table 1: Data used for the analysis thermodynamic analysis

Input Parameter	Value
Place	Cape Town (South Africa)
Solar collector field efficiency parameters	$\eta_{o,CL}$ = 0.833; U_l = 0.85 W/(m^2·K) and 0.68 W/(m^2·K) (with improvements)
Specific land requirement	3.5·A_p
Solar collector field heat transfer fluid	Therminol VP-1
Storage heat transfer fluid	Hitec XL
Storage tank UA	0.00017·T_{salt} + 0.012 (kW/m^2); T_{salt} is the temperature of salt (°C) (Herrmann *et al.*, 2004)
Design condition ambient temperature (T_a)	30°C
Gross peak plant output at design ($P_{gross,D}$)	1 MWe
Penalty for start-up/shut-down and other losses	10 % of net power output (Manzolini *et al.*, 2011)
Parasitic electric energy use for solar field, TES pump, antifreeze pumping	7 % of net power output (NREL, 2018)
Electricity consumption of MED system	1 kWh$_e$/m^3 (Alfa Laval, 2018)
Thermal energy requirement of MED system	120 kWh$_{th}$/m^3 (Alfa Laval, 2018)
TES electric heating system efficiency	0.9
Temperature driving force at design (ΔT_{min})	20°C (for regenerator); 5°C (for condenser)
Turn down ratio of turbine (P_{min}/P_{max})	0.1 (Turboden, 2018)
Generator efficiency parameters ($\eta_{g,D}$)	$\eta_{g,D}$ = 0.93
Isentropic efficiency of pump ($\eta_{P,D}$)	$\eta_{P,D}$ = 0.7

Table 2: Data used for the economic analysis

Parameters	Value
Solar field and heat transfer fluid system cost (€)	250 (for current plants) and 150 (for future plants)
Land and site development cost (€/m^2 of land)	4.7 (IIT Bombay, 2014)
Specific cost of Hitec XL (€/kg)	0.93 (Pan *et al.*, 2018)
Storage tank cost (including insulation and foundation) (€/m^3)	$\frac{C_{ST,Tank}}{C_{ref,Tank}} = \left(\frac{Capacity_{ST,Tank}}{Capacity_{ref,Tank}}\right)^{0.85}$; $C_{ref,Tank}$ = 7,932,160 € (Herrmann *et al.*, 2004), $Capacity_{ref,Tank}$ = 30,844 m^3 (Herrmann *et al.*, 2004)
Oil to salt heat exchanger cost (€)	$\frac{C_{ST,HX}}{C_{ref,HX}} = \left(\frac{Capacity_{ST,HX}}{Capacity_{ref,HX}}\right)^{0.85}$; $C_{ref,HX}$ = 4,580,235 € (Herrmann *et al.*, 2004), $Capacity_{ref,HX}$ = 133 MW$_{th}$ (Herrmann *et al.*, 2004)
Balance of storage system and salt pump cost (€)	14 % of the storage system cost (Herrmann *et al.*, 2004)
Civil works cost (€)	133·(kW_e) – 0.00042·(kW_e)$^{0.75}$ (Krishnamurthy *et al.*, 2012)
Miscellaneous cost (€/kW$_e$)	144 (IIT Bombay, 2014)
Evaporator and regenerator cost (€)	$C_0 \cdot \left(\frac{UA}{UA_0}\right)^{0.9} \cdot a$; $a = (10)^{(a_1 + a_2 \cdot \log Pr + a_3 \cdot log^2 Pr)}$; For evaporator: C_0 = 1570 k€, a_1 = 0.03881, a_2 = – 0.11272, a_3 = 0.08183; For regenerator: C_0 = 272 k€, a_1 = – 0.00164, a_2 = – 0.00627, a_3 = 0.0123 (Astolfi *et al.*, 2014)
Turbine cost (€)	$1{,}287{,}810 \cdot \left(\frac{n}{n_{ref}}\right)^{0.85} \cdot \left(\frac{SP}{SP_{ref}}\right)^{1.1}$; n = number of stages, SP = last stage size parameter, n_{ref} = 2, SP_{ref} = 0.18 m (Astolfi *et al.*, 2014)
Generator cost (€)	$209{,}400 \cdot \left(\frac{kW_e}{5{,}000}\right)^{0.67}$ (Astolfi *et al.*, 2014)
Gear box cost (€)	40 % of the generator cost (Astolfi *et al.*, 2014)
Condenser cost (€)	$13{,}075 \cdot \left(\frac{kW_{th}}{50}\right)^{0.76}$ (Lemmens, 2016)
Boiler feed pump cost (€)	$14{,}658 \cdot \left(\frac{kW}{200}\right)^{0.67}$ (Astolfi *et al.*, 2014)
Balance of power system	40 % of the power system equipment cost (Astolfi *et al.*, 2014)
Capital cost of MED system (€/(m^3·d))	1500
Annual operating and maintenance cost	Fixed cost (on total investment) – 1.4 %; Variable cost – 2.8 €/MWh$_e$
Lifetime (y)	25

Note: Parameters for cost correlations have been updated to the monetary value of 2018 using the Chemical Engineering Plant Cost Index. For the conversion of $ to €, the annual average exchange rate for the particular year was used.

highest limit of the evaporation temperature suggested by Rayegan and Tao (2011). The superheating degree at turbine inlet was varied from 0 °C to 40 °C. Figure 2 shows the effects of variations in degree of superheat for current plants. With increase in degree of superheat the power cycle thermal efficiency increases; however, the solar collector field efficiency decreases because of increase in the average temperature of heat addition. Due to higher increase in the power cycle efficiency compared to the decrease in the solar collector field efficiency, the resulting overall system efficiency increases. As a result, the solar collector field area requirement decreases (see Figure 2a). For a fixed number of turbine stages, the power block cost decreases with increase in degree of superheat. In the present analysis, the maximum isentropic enthalpy drop per stage of the ORC turbine is considered as 65 kJ/kg (Astolfi *et al.*, 2014). Therefore, for the organic working fluids MM and isopentane, the number of stages changes at 15 °C and at 20 °C degree of superheat, resulting in a sudden increase in the power block cost for these fluids (see Figure 2b). The storage system cost decreases with the increase in degree of superheat (see Figure 2c), because the requirement of the molten salt decreases significantly with increase in operating temperature difference of the storage system. Based on the variations in the solar field cost, power block cost and storage system cost, the total capital cost also changes (see Figure 2d). Similar trends are obtained also for the future plants based on the foil-based concentrating solar field (see Figure 3).

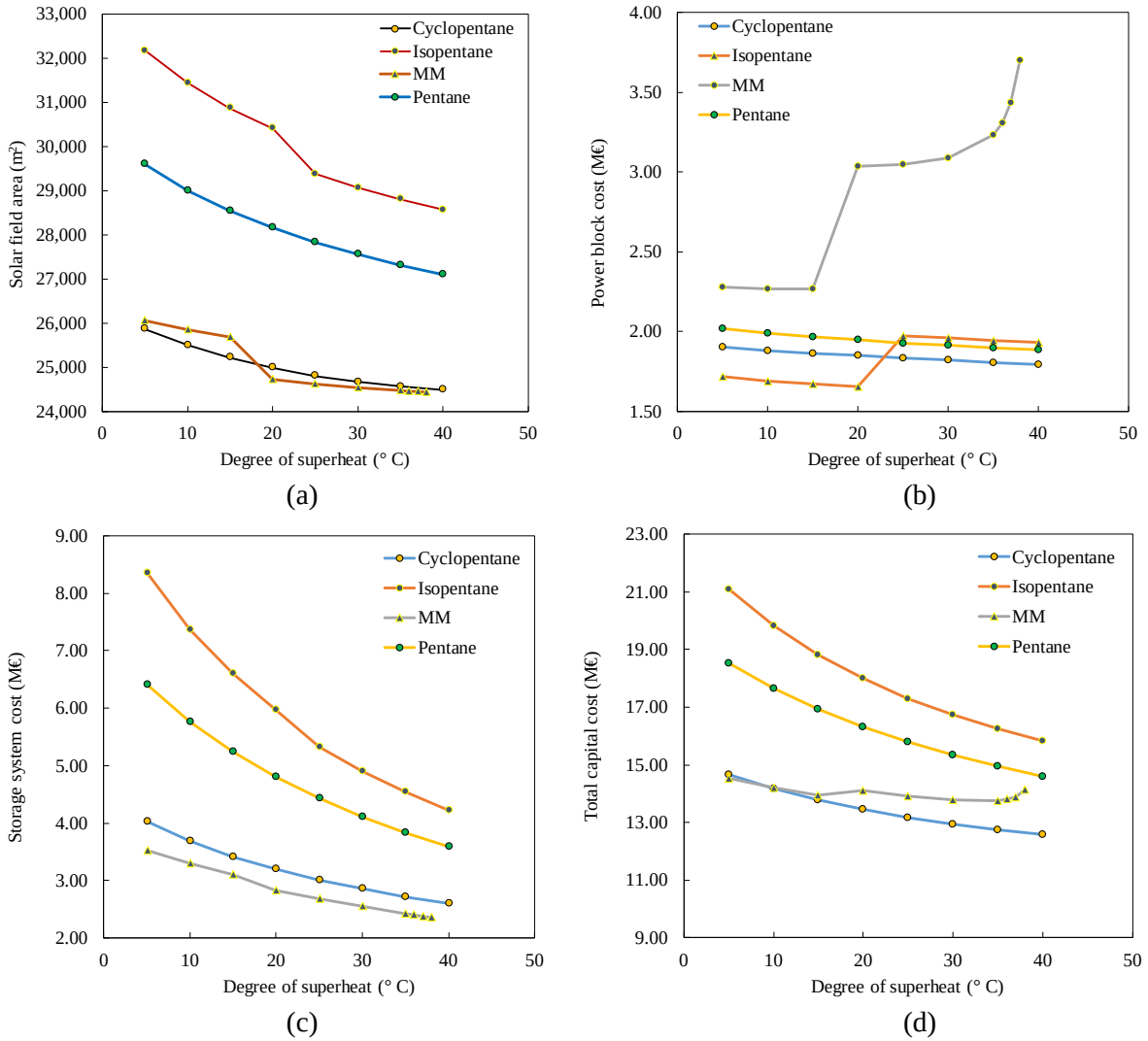

Figure 2: Effects of variations in degree of superheat for turbine inlet temperature for current plants on (a) solar collector field area, (b) power block cost, (c) storage system cost, and (d) total capital cost.

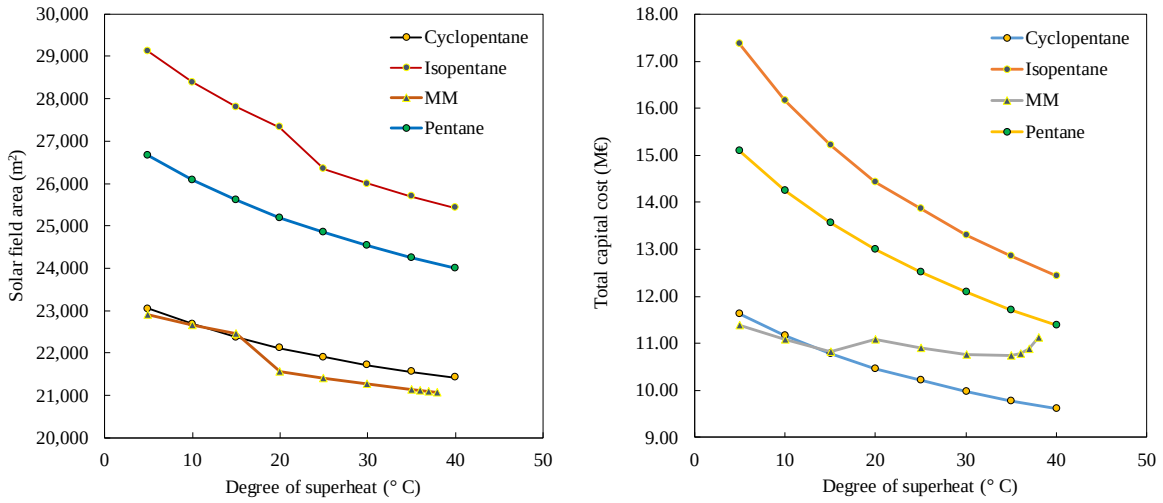

(a) (b)

Figure 3: Effects of variations in degree of superheat for turbine inlet temperature for future plants on (a) solar collector field area, and (b) total capital cost.

Table 3: Results of a techno-economic analysis of the system (1 MW_e plant with 9 h storage capacity)

Parameters	Cyclopentane		MM		N-Pentane		Isopentane	
	Current plants	Future plants	Current plants	Future plants	Current plants	Future plants	Current plants	Future plants
Critical pressure, P_{crit} (MPa)	4.571		1.939		3.37		3.378	
Critical temperature, T_{crit} (°C)	238.6		245.5		196.6		187.2	
Solar field inlet temperature, $T_{in,CL}$ (°C)	167.3		175.7		165		165	
Solar field outlet temperature, $T_{out,CL}$ (°C)	278		290		256		247	
Evaporator pressure, P_{eva} (MPa)	2.569		1.201		2.467		2.464	
Evaporator outlet temperature, $T_{out,eva}$ (°C)	238		250		216		207	
Solar collector field area, $A_{p,CL}$ (m^2)	24,498	21,418	24,476	21,148	27,098	24,004	28,567	25,423
MED system capacity (m^3/day)	908		862		1,087		1,180	
Net annual electricity generation (MWh_e/y)	2,899	2,887	2,845	2,825	2,823	2,810	2,722	2,690
Annual fresh water generation (m^3/y)	149,617	149,053	139,070	138,361	181,111	180,340	200,371	199,509
LCOE (€/kWh_e)	0.224	0.176	0.277	0.226	0.238	0.188	0.255	0.206
LCOW (€/m^3)	1.74	1.27	1.48	1.02	2.12	1.65	2.24	1.75

For the techno-economic analysis of the foil-based collector powered ORC integrated MED system, the value of degree of superheat corresponding to the lowest capital cost was selected for all working fluids. In order to determine the optimum value of LCOE and LCOW (for a given place, solar collector field and storage capacity), the variations with respect to solar field area were determined and optimized values are reported in the Table 3. Results considering medium to large-scale production cost (150 €/m^2) and 20 % improvement in the heat-loss coefficient of the receiver, is also presented (see Table 3). The results suggest that cyclopentane achieves the lowest LCOE (for current plants: 0.224 €/kWh, for future plants: 0.176 €/kWh) and MM achieves lowest levelized cost of fresh water generation (LCOW) (for current plants: 1.48 €/m^3, for future plants: 1.02 €/m^3). From a techno-economic perspective, considering both electricity and fresh water generation, the results indicate that cyclopentane is the preferred working fluid among the ones considered in the analysis.

It needs to be stressed that the final selection of working fluid also needs to consider other aspects of the working fluids that were not considered in this analysis (e.g. environmental, health, safety and legislative aspects). Moreover, it is worth to note that the amount of fresh water generation at design condition also decreases because of higher power block efficiency with increase in the degree of superheat. This will result in decrease in the annual fresh water generation. Therefore, the final selection of the optimum value of the degree of superheat should be done based on the lowest value of LCOE and LCOW. Conducting optimizations considering the effects on the annual performances of variations in the degree of superheat and other relevant parameters are the subject of future work.

4. CONCLUSIONS

In this paper, a comparative analysis among different organic working fluids for micro-structured polymer foil-based concentrated solar power plants for electricity and fresh water generation was performed. For medium-scale applications (few hundreds kW_e to few MW_e) for dispatchable power and fresh water generation, a concentrated solar power based organic Rankine cycle system integrated with multi-effect distillation unit is the preferred option. The results suggest that cyclopentane is the preferred working fluid. For a foil-based concentrated solar power plant with cyclopentane, the levelized cost of electricity (for current plants as well as future plants) is about 5.9–6.4 % and 19.1–22.1 % lower compared to n-pentane and hexamethyldisiloxane-based plants, respectively. The levelized cost of water (for current as well as future plants) for cyclopentane-based plants is 17.6–24.5 % higher compared to hexamethyldisiloxane based plants and 17.9–23 % lower compared to n-pentane based plants. The foil-based concentrating solar power system is a promising alternative for cogeneration and multi-generation plants.

REFERENCES

Alfa Laval, 2018, <www.alfalaval.com/globalassets/documents/products/process-solutions/desalination-solutions/multi-effect-desalination/fresh-water-brochure-pee00251en-1201.pdf>, accessed 01.07.18.

Astolfi, M., Macchi, E., 2015, Efficiency correlations for axial flow turbines working with non-conventional fluids. *In Proceedings of the 3rd International Seminar on ORC Power Systems*, Brussels, Belgium: pp. 12-14.

Astolfi, M., Mazzola, S., Silva, P., Macchi, E., 2017, A synergic integration of desalination and solar energy systems in stand-alone microgrids, *Desalin*, vol. 419: pp.169-180.

Astolfi, M., Romano, M.C., Bombarda, P., Macchi, E., 2014, Binary ORC (Organic Rankine Cycles) power plants for the exploitation of medium–low temperature geothermal sources–Part B: Techno-economic optimization, *Energy*, 66: pp. 435-446.

Bandyopadhyay, S., Desai, N.B., 2016, Cost optimal energy sector planning: a Pinch Analysis approach, *J Clean Prod*, 136: pp. 246-253.

Bruno, J.C., Lopez-Villada, J., Letelier, E., Romera, S., Coronas, A., 2008, Modelling and optimisation of solar organic rankine cycle engines for reverse osmosis desalination, *Appl Therm Eng*, vol. 28(17-18): pp. 2212-2226.

Delgado-Torres, A.M., García-Rodríguez, L., 2007, Comparison of solar technologies for driving a desalination system by means of an organic Rankine cycle. *Desalin*, 216(1-3), pp. 276-291.

Desai, N.B., Kedare S.B., Bandyopadhyay S., 2014, Optimization of design radiation for concentrating solar thermal power plants without storage. *Sol Energy*, vol. 107: pp. 98–112.

Desai, N.B., Pranov, H., Haglind, F., 2019, Techno-economic analysis of a power generation system consisting of a foil-based concentrating solar collector and an organic Rankine cycle unit. *In Proceedings of the 32nd International conference on efficiency, cost, optimization, simulation and environmental impact of energy systems (ECOS 2019).* (Accepted for publication).

Heller, P. (editor), 2017, The Performance of Concentrated Solar Power (CSP) Systems: Analysis, Measurement and Assessment. Woodhead Publishing.

El-Emam, R.S., Dincer, I., 2018, Investigation and assessment of a novel solar-driven integrated energy system. *Energy Convers Manage*, vol. 158: pp. 246-255.

Ghobeity, A., Noone, C.J., Papanicolas, C.N., Mitsos, A., 2011, Optimal time-invariant operation of a power and water cogeneration solar-thermal plant, *Sol Energy*, vol. 85: pp. 2295–2320.

Gutiérrez-Arriaga, C.G., Abdelhady, F., Bamufleh, H.S., Serna-González, M., El-Halwagi, M.M., Ponce-Ortega, J.M., 2015, Industrial waste heat recovery and cogeneration involving organic Rankine cycles, *Clean Technologies and Environmental Policy*, vol. 17(3): pp.767-779.

Haglind, F., Elmegaard, B., 2009, Methodologies for predicting the part-load performance of aero-derivative gas turbines. *Energy*, vol. 34(10): pp. 1484–1492.

Hasselmann, K., Reinker, F., Wiesche, S., Kenig, E.Y., Dubberke, F. and Vrabec, J., 2014, Performance Predictions of Axial Turbines for Organic Rankine Cycle (ORC) Applications Based on Measurements of the Flow Through Two-Dimensional Cascades of Blades. In ASME 2014 Power Conference, American Society of Mechanical Engineers.

Herrmann, U., Kelly, B., Price, H., 2004, Two-tank molten salt storage for parabolic trough solar power plants. *Energy*, vol. 29(5-6): pp. 883–893.

Hoffmann, J.E., Dall, E.P., 2018, Integrating desalination with concentrating solar thermal power: Namibian case study, *Renew. Energy*, vol. 115: pp. 423–432.

IIT Bombay, 2014 Solar Thermal Simulator Version 2.0.

IRENA, 2012. Water Desalination Using Renewable Energy.

Karellas, S., Terzis, K., Manolakos, D., 2011, Investigation of an autonomous hybrid solar thermal ORC–PV RO desalination system. The Chalki island case, *Renew Energy*, vol. 36(2):pp. 583-590.

Klein, S., 2018. "Software F-Chart, EES-Engineering Equation Solver" V10.478.

Krishnamurthy P., Mishra S., Banerjee R., 2012, An analysis of costs of parabolic trough technology in India, *Energy Policy*, vol. 48: pp. 407–419.

Lemmens, S., 2016, Cost engineering techniques and their applicability for cost estimation of organic Rankine cycle systems. *Energies*, vol. 9(7): pp. 485.

Li, C., Kosmadakis, G., Manolakos, D., Stefanakos, E., Papadakis, G., Goswami, D.Y., 2013, Performance investigation of concentrating solar collectors coupled with a transcritical organic Rankine cycle for power and seawater desalination co-generation. *Desalin*, vol. 318: pp. 107-117.

Manzolini, G., Bellarmino, M., Macchi, E., Silva, P., 2011, Solar thermodynamic plants for cogenerative industrial applications in southern Europe, *Renew Energy*, vol. 36(1): pp. 235–243.

Mathkor, R., Agnew, B., Al-Weshahi, M., Latrsh, F., 2015, Exergetic analysis of an integrated tri-generation organic Rankine cycle, *Energies*, vol. 8(8): pp. 8835-8856.

Mavromatis S.P., Kokossis A.C., 1998, Conceptual optimisation of utility networks for operational variations—I. targets and level optimisation. *Chem Eng Sci*, vol. 53: pp. 1585–1608.

NREL, 2018. National Renewable Energy Laboratory, <www.sam.nrel.gov/> accessed 15.12.2018.

NREL, 2019. <www.nrel.gov/csp/solarpaces/by_status.cfm>, accessed 21.01.19.

Palenzuela, P., Alarcón-Padilla, D.C., Zaragoza, G., Blanco, J., 2015, Comparison between CSP+MED and CSP+RO in Mediterranean area and MENA region: techno-economic analysis, *Energy Procedia*, vol. 69: pp. 1938–1947.

Pan, C.A., Ferruzza, D., Guédez, R., Dinter, F., Laumert, B., Haglind, F., 2018, Identification of optimum molten salts for use as heat transfer fluids in parabolic trough CSP plants: A techno-economic comparative optimization. *In AIP Conference Proceedings*, vol. 2033(1): pp. 030012.

Patil, V.R., Biradar, V.I., Shreyas, R., Garg, P., Orosz, M.S., Thirumalai, N.C., 2017, Techno-economic comparison of solar organic Rankine cycle (ORC) and photovoltaic (PV) systems with energy storage, *Renew energy*, 113: pp. 1250-1260.

Patnode, A.M., 2006, Simulation and performance evaluation of parabolic trough solar power plants. M.Sc. Thesis, University of Wisconsin-Madison.

Rayegan R., Tao Y.X., 2011, A procedure to select working fluids for solar organic Rankine cycles (ORCs), *Renew energy*, 36: pp. 659–670.

Shalaby, S.M., 2017, Reverse osmosis desalination powered by photovoltaic and solar Rankine cycle power systems: a review, *Renew Sustain Energy Rev*, 73: pp.789-797.

Sharaf, M.A., 2012, Thermo-economic comparisons of different types of solar desalination processes. *J Sol Energy Eng*, vol. 134(3): p. 031001.

Sharan, P., Neises, T., McTigue, J. D., Turchi, C., 2019, Cogeneration using multi-effect distillation and a solar-powered supercritical carbon dioxide Brayton cycle, *Desalin*, vol. 459: p. 20-33.

Turboden, 2018. <www.turboden.com> accessed 22.11.2018.

US DOE (2014) Energy Plus Energy Simulation Software, Energy Efficiency and Renewable Energy.
Veres, J., 1994, Centrifugal and Axial Pump Design and Off-Design Performance Prediction; Technical Report; NASA: Sunnyvale, CA, USA.

ACKNOWLEDGEMENT

The research presented in this paper has been funded by the European Union's Horizon 2020 research and innovation programme with a Marie Skłodowska-Curie Individual Fellowship under grant agreement no. 794562 (Project: Small-scale CSP). The financial support is gratefully acknowledged.